

Results From the NA62 Experiment at CERN



Mattia Soldani

1 Introduction

Over the last seven decades, measurements of kaon decays have played a central role in both testing the Standard Model (SM) and searching for New Physics (NP). Indeed, the kaon sector proves a powerful probe at the intensity frontier, owing to a small number of decay modes, to rather simple final states and to the accessibility of intense kaon beams [7].

The NA62 experiment is currently carrying on the successful series of kaon decay experiments at the CERN North Area [4]. It makes use of a 400 GeV/ c primary proton beam extracted from the CERN Super Proton Synchrotron with $(1.9\text{--}2.2) \times 10^{12}$ protons per (~ 4.8 s long) pulse and a relative duty cycle of

Mattia Soldani, on behalf of the NA62 Collaboration: A. Akmete, R. Aliberti, F. Ambrosino, R. Ammendola, B. Angelucci, A. Antonelli, G. Anzivino, R. Arcidiacono, T. Bache, A. Baeva, D. Baigarashev, L. Bandiera, M. Barbanera, J. Bernhard, A. Biagioni, L. Bician, C. Biino, A. Bizzeti, T. Blazek, B. Bloch-Devaux, P. Boboc, V. Bonaiuto, M. Boretto, M. Bragadireanu, A. Briano Olvera, D. Britton, F. Brizioli, M.B. Brunetti, D. Bryman, F. Bucci, T. Capussela, J. Carmignani, A. Ceccucci, P. Cenci, V. Cerny, C. Cerri, B. Checcucci, A. Conovaloff, P. Cooper, E. Cortina Gil, M. Corvino, F. Costantini, A. Cotta Ramusino, D. Coward, P. Cretaro, G. D'Agostini, J. Dainton, P. Dalpiaz, H. Danielsson, M. D'Errico, N. De Simone, D. Di Filippo, L. Di Lella, N. Doble, B. Dobrich, F. Duval, V. Duk, D. Emelyanov, J. Engelfried, T. Enik, N. Estrada-Tristan, V. Falaleev, R. Fantechi, V. Fascianelli, L. Federici, S. Fedotov, A. Filippi, R. Fiorenza, M. Fiorini, O. Frezza, J. Fry, J. Fu, A. Fucci, L. Fulton, E. Gamberini, L. Gatignon, G. Georgiev, S. Ghinescu, A. Gianoli, M. Giorgi, S. Giudici, F. Gonnella, K. Gorsharov, E. Goudzovski, C. Graham, R. Guida, E. Gushchin, F. Hahn, H. Heath, J. Henshaw, Z. Hives, E.B. Holzer, T. Husek, O. Hutanu, D. Hutchcroft, L. Iacobuzio, E. Iacopini, E. Imbergamo, B. Jenninger, J. Jerhot, R.W. Jones, K.

M. Soldani (✉)

INFN Laboratori Nazionali di Frascati, Frascati, Italy

© The Author(s) 2026

Y. Tayalati, M. Gouighri (eds.), *The First African Conference on High Energy*

Physics, Springer Proceedings in Physics 425,

https://doi.org/10.1007/978-3-031-88933-2_25

~ 0.3 [7]. The primary beam impinges on a beryllium target, thus producing a secondary, unseparated positive hadron beam, with a total rate of 750 MHz consisting of approximately 70% charged pions, 23% protons and 6% charged kaons. The $75 \text{ GeV} \pm 1\%$ momentum component of the secondary beam is used by the experiment [7].

The NA62 apparatus essentially consists of an instrumented 117 m long vacuum tank, with variable diameter between 1.92 m (upstream) and 2.8 m (downstream). It was designed with a strong focus on excellent time resolution for matching the incident kaon and the decay output tracks with a precision of $\mathcal{O}(100 \text{ ps})$; a powerful and redundant charged-particle identification (PID) system; a highly hermetic coverage of the decay volume, to guarantee that the full reconstruction of both the signal kinematics and the background veto (especially the channels with final-state photons from π^0 decays) is performed with high efficiency [7].

Firstly, the kaon component of the secondary beam is identified with high efficiency ($\gtrsim 99\%$) by the KTAG (Kaon TAGger) [22], a CEDAR (ChErenkov Differential counter with Achromatic Ring focus) derived from the CERN CEDAR-W design with custom photodetection and readout systems. The track and momentum of the beam particle is also measured with a beam spectrometer, the Giga TracKer (GTK) [27], which consists of an array of silicon pixel modules installed around 4 dipole magnets arranged as a magnetic achromat. Each module is $510 \mu\text{m}$ thick, with a $300 \times 300 \mu\text{m}^2$ pixel pitch. Overall, an angular resolution of $16 \mu\text{rad}$ and a relative momentum resolution of 0.2% are attained.

The fiducial volume (FV), i.e., the region in which the kaon primary decay vertices are sought, occupies the first 60 m of the vacuum tank, downstream of the GTK. Only about 4.5 MHz of charged kaons, i.e., 10% of those entering the experiment, decay in the FV. Several subsystems are devoted to the measurement of the decay products. A brief summary of the main elements of the apparatus is provided in the following. Further details can be found in Ref. [7].

Kampf, V. Kekelidze, D. Kereibay, S. Kholodenko, G. Khoriauli, A. Khotyantsev, A. Kleimenova, A. Korotkova, M. Koval, V. Kozhuharov, Z. Kucerova, Y. Kudenko, J. Kunze, V. Kurochka, V. Kurshtsov, G. Lanfranchi, G. Lamanna, E. Lari, G. Latino, P. Laycock, C. Lazzeroni, M. Lenti, G. Lehmann Miotto, E. Leonardi, P. Lichard, L. Litov, P. Lo Chiatto, R. Lollini, D. Lomidze, A. Lonardo, P. Lubrano, M. Lupi, N. Lurkin, D. Madigozhin, I. Mannelli, A. Mapelli, F. Marchetto, R. Marchevski, S. Martellotti, P. Massarotti, K. Massri, E. Maurice, A. Mazzolari, M. Medvedeva, A. Mefodev, E. Menichetti, E. Migliore, E. Minucci, M. Mirra, M. Misheva, N. Molokanova, M. Moulson, S. Movchan, M. Napolitano, I. Neri, F. Newson, A. Norton, M. Noy, T. Numao, V. Obraztsov, A. Okhotnikov, A. Ostankov, S. Padolski, R. Page, V. Palladino, I. Panichi, A. Parenti, C. Parkinson, E. Pedreschi, M. Pepe, M. Perrin-Terrin, L. Peruzzo, P. Petrov, Y. Petrov, F. Petrucci, R. Piandani, M. Piccini, J. Pinzino, I. Polenkevich, L. Pontisso, Yu. Potrebenikov, D. Protopopescu, M. Raggi, M. Reyes Santos, M. Romagnoni, A. Romano, P. Rubin, G. Ruggiero, V. Ryjov, A. Sadovsky, A. Salamon, C. Santoni, G. Saracino, F. Sargeni, S. Schuchmann, V. Semenov, A. Sergi, A. Shaikhiev, S. Shkarovskiy, M. Soldani, D. Soldi, M. Sozzi, T. Spadaro, F. Spinella, A. Sturgess, V. Sugonyaev, J. Swallow, A. Sytov, G. Tinti, A. Tomczak, S. Trilov, M. Turisini, P. Valente, B. Velghe, S. Venditti, P. Vicini, R. Volpe.

The charged particle trajectories are reconstructed by a magnetic spectrometer, which includes a bending magnet [21] (with a transverse momentum kick of 270 MeV/c) instrumented by 4 straw-tube modules [7] (STRAW) with a spatial resolution of 130 μm and a momentum resolution of $0.3\% + 0.005\%p$ (p being the particle momentum), together with a Charged-particle HODoscope (CHOD) [25].

A hermetic photon-veto system provides efficient coverage to the detection of photons from several background sources in a very wide angular range. In particular, the Large-Angle Veto (LAV) [1] encompasses 12 modules of ring-shaped arrays of lead glass blocks, deployed around and downstream of the FV, providing an angular coverage up to 50 mrad. On the other hand, angles ≤ 8.5 mrad are covered by electromagnetic calorimeters placed at the downstream end of the apparatus: the NA48 Liquid Krypton (LKr) calorimeter [20], the Intermediate-Ring Calorimeter (IRC) and the Small-Angle Calorimeter (SAC) [7]. Overall, a π^0 suppression at the level of 10^{-8} is achieved.

Hadronic calorimeters [7, 20] and a Ring-Image Cherenkov Detector (RICH) [2, 3] allow for a powerful PID. Overall, a muon suppression at the level of 10^{-7} is achieved. Moreover, the RICH provides a high-time-resolution (< 100 ps) reference for the output state [3] and allows for additional muon-pion separation at the level of 10^{-2} .

2 $K^+ \rightarrow \pi^+ \nu \bar{\nu}$ and $K^+ \rightarrow \pi^+ X$

The $K^+ \rightarrow \pi^+ \nu \bar{\nu}$ (PNN) decay (as well as its neutral counterpart, $K_L \rightarrow \pi^0 \nu \bar{\nu}$) is a flavor-changing neutral current process that proceeds via Z -penguin and double- W -box diagrams [7]. It is heavily suppressed because of the GIM mechanism and of the CKM hierarchy, with a branching ratio $\text{BR}_{\text{PNN}}^{\text{SM}} = (7.86 \pm 0.61) \times 10^{-11}$ in the SM [18]. See also, e.g., [5, 6]. As the decay dynamics is dominated by short-distance contributions and its hadronic matrix element can be obtained from the experimental measurement of the K_{e3} channel ($K^+ \rightarrow \pi^0 e^+ \nu_e$) with sub-% precision, rather clean theoretical predictions are accessible in the SM. The $K^+ \rightarrow \pi^+ \nu \bar{\nu}$ decay may prove highly sensitive to flavor NP, including, e.g., non-SM behaviour due to new sources of flavor violation, direct CP violation, lepton-flavor non-universality and leptoquarks [7].

Essentially, the PNN reconstruction proceeds by identifying an input K^+ track that matches an output π^+ track with some missing transverse momentum (due to the neutrinos) with the decay vertex inside the FV. In the $(p_\pi, m_{\text{miss}}^2)$ plane two boxes are identified as the signal region (Fig. 1 left) and several other regions are defined for validation and evaluation of three of the main background sources, i.e., $K^+ \rightarrow \mu^+ \nu_\mu$, $K^+ \rightarrow \pi^+ \pi^+ \pi^-$ and $K^+ \rightarrow \pi^+ \pi^0$; the latter is also used as a normalization channel. Two other contributions to the overall background are noteworthy: the one from $K^+ \rightarrow \pi^+ \pi^- e^+ \nu_e$, which only affects the signal box at higher m_{miss}^2 and was characterized with simulations only, and the so-called upstream background, given by π^+ coming from K^+ interactions or decay in flight

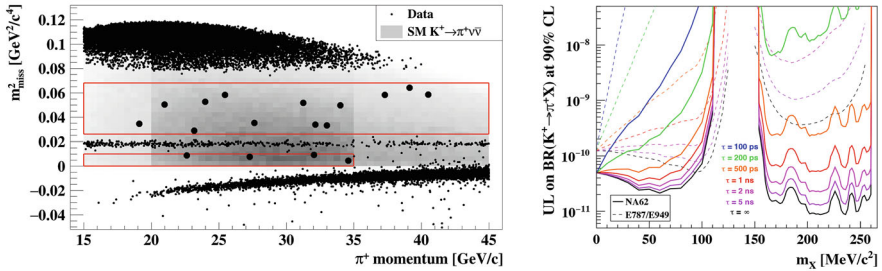


Fig. 1 *Left*: PNN candidate events from the 2018 dataset in the $(p_\pi, m_{\text{miss}}^2)$ plane. The intensity of the gray shaded area reflects the variation of the SM signal acceptance. The signal regions are highlighted in red. *Right*: Model-independent observed BR upper limits for different X mass and lifetime hypotheses. Reprinted under CC-BY-4.0 license from Ref. [10]. © 2021, CERN for the benefit of the NA62 Collaboration

occurring upstream of the FV, which was characterized with a data-driven approach. The analysis procedure is described in extensive detail in Refs. [8–10].

The datasets collected in 2016 [8], 2017 [9] and 2018 [10] (in Fig. 1 left) have been analyzed. Overall, a single-event sensitivity of $(0.839 \pm 0.053_{\text{sys}}) \times 10^{-11}$ has been reached [10]. 20 candidate events have been observed in the signal region, to be compared to the expected sum of $10.01 \pm 0.42_{\text{sys}} \pm 1.19_{\text{ext}}$ PNN events and $7.03^{+1.05}_{-0.82}$ background events [10]. This leads to $\text{BR}_{\text{PNN}}^{\text{meas}} = (10.6^{+4.0}_{-3.4} |_{\text{stat}} \pm 0.9_{\text{sys}}) \times 10^{-11}$ at 68% CL, which is the most precise measurement to date, and corresponds to 3.4σ evidence for the existence of the decay channel [10].

The event sample selected in the PNN analysis has been used to search for evidence of the $K^+ \rightarrow \pi^+ X$ decay, where X is a dark scalar or pseudo-scalar. X can be stable, decay to other invisible particles or live long enough to decay outside the NA62 apparatus. This search proceeds under the assumption that all the events observed in the PNN signal regions correspond to the expected background—i.e., including the PNN events, which in this case constitute the main background source. As shown in Fig. 1 right, upper limits are established on $\text{BR}(K^+ \rightarrow \pi^+ X)$ for different X mass and lifetime hypotheses. Further details can be found in Ref. [10].

3 $K^+ \rightarrow \pi^+ e^+ e^- e^+ e^-$

In the SM, the $K^+ \rightarrow \pi^+ e^+ e^- e^+ e^-$ decay proceeds mainly through the $\pi^+ \pi^0$ state followed by the double-Dalitz $\pi^0 \rightarrow e^+ e^- e^+ e^-$ decay (“ $K_{2\pi\text{DD}}$ ”), which is resonant and has a branching ratio $\text{BR}_{2\pi\text{DD}}^{\text{meas}} = (6.9 \pm 0.3) \times 10^{-6}$ [23]. This final state also features a non-resonant contribution (“ $K_{\pi 4e}$ ”), given by an intermediate state with a one-/two-photon exchange and with a branching ratio $\text{BR}_{2\pi\text{DD}}^{\text{theo}} = (7.2 \pm 0.7) \times 10^{-11}$ in the SM [17].

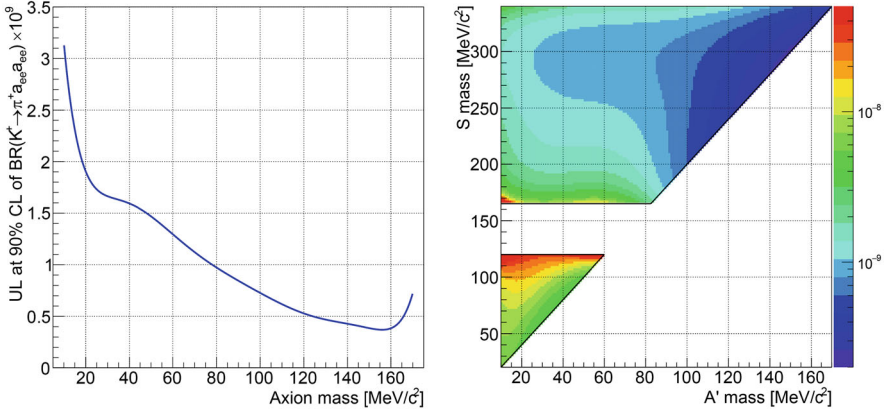


Fig. 2 Upper limits at 90% CL of the decay chains $K^+ \rightarrow \pi^+ aa \rightarrow \pi^+ e^+ e^- e^- e^-$ (left) and $K^+ \rightarrow \pi^+ S \rightarrow \pi^+ A' A' \rightarrow \pi^+ e^+ e^- e^- e^-$ (right) as a function of the masses of the dark mediators involved. Reprinted under CC-BY-4.0 license from [17]. © 2023, The Author(s)

The $K_{\pi 4e}$ channel is also a suitable probe for the dark sector. In particular, the decay might proceed through the $K^+ \rightarrow \pi^+ aa$ state, where a is a dark axion decaying into an electron-positron pair. Moreover, a scenario involving an intermediate state with a dark scalar S that decays into two dark photons A' , which in turn decay into an electron-positron pair each, is considered.

The rather characteristic kinematics of the final state allows for this analysis to rely exclusively on the STRAW data, which prevents an approximately tenfold loss of signal acceptance. Omitting the information from the other detectors in the apparatus reduces the selectivity, which is feasible because strong kinematic constraints can be used. The $K_{2\pi DD}$ channel is used for normalization, whereas the signal events are sought in the non-resonant part. Extensive details of the event selection procedure are provided in Ref. [17].

The analysis was performed on the 2017–2018 data. No signal candidates were observed within the signal selection cuts [17]. This corresponds to the upper limit $\text{BR}_{\pi 4e}^{\text{meas}} < 1.4 \times 10^{-8}$ at 90% CL, which is ~ 200 times larger than the SM expectation [17]. Upper limits were also estimated for decay chains initiating from axions and scalar dark-sector particles, as a function of the masses of the dark mediators involved: they are shown in Fig. 2. In particular, the QCD axion model is excluded as a possible explanation of the $X17$ observations [26].

4 $K^+ \rightarrow \mu^- \nu e^+ e^+$

Depending on the flavor of the neutrino, the $K^+ \rightarrow \mu^- \nu e^+ e^+$ (“ $K_{\mu \nu ee}$ ”) decay violates conservation of either lepton flavour or both lepton flavour and lepton

number. NA62 searched for evidence of this decay in the data collected between 2016 and 2018. Details of the analysis can be found in Ref. [14].

No signal candidates were found within the signal selection box, which leads to the upper limit $\text{BR}_{\mu\nu e e}^{\text{meas}} < 8.1 \times 10^{-11}$ at 90% CL [14]. This also corresponds to a 250-fold improvement of the result of previous searches [19].

5 $A' \rightarrow \mu^+ \mu^-$ in Beam-Dump Mode

A search for evidence of the $A' \rightarrow \mu^+ \mu^-$ decay, where A' is a dark photon with a mass of $\mathcal{O}(100 \text{ MeV})$, can be made by running the NA62 experiment in dump mode. In this mode, which is described in detail in Ref. [16], the 400 GeV/c protons from the Super Proton Synchrotron directly impinge on the fully-closed hadron beam collimators (TAXes—800 mm of copper and 2400 mm of iron).

About 10 days of dump-mode run were performed in 2021. The resulting data were used to search for the aforementioned decay, as discussed in Ref. [16]. One event passed the signal selection criteria, which would correspond to a 2.4σ global significance [16]. This event could be interpreted as background, as it is located close to the border of the signal selection cuts; indeed, the probability of background observation within the signal region is 1.6% [16]. Overall, no evidence of the decay under study is established [16].

6 Conclusions and Outlook

The NA62 experiment is currently very active in exploring the kaon sector. Firstly, the PNN decay channel, for which an evidence at the level of 3.4σ was reached, is being thoroughly characterized. Moreover, numerous searches for NP through dark mediators, such as in $K^+ \rightarrow \pi^+ X$, in $K^+ \rightarrow \pi^+ e^+ e^- e^+ e^-$ and in $A' \rightarrow \mu^+ \mu^-$ (measured in dump mode), and lepton-flavour/number-violating processes like $K^+ \rightarrow \mu^- \nu e^+ e^+$ are being performed. Other searches done by the NA62 experiment are discussed in Refs. [12, 13, 15]. No evidence of deviations from the SM have been found so far.

At the same time, the HIKE (High Intensity Kaon Experiments) experiment [11, 24] is under development, with the aim of succeeding NA62 after the end of its operations, expected in late 2025, bringing charged-kaon measurements to an unprecedented sensitivity level and extending the kaon program at CERN to K_L physics.

References

1. A. Antonelli et al., Performance of the NA62 LAV front-end electronics. *J. Instrum.* **8**(01), C01020 (2013). <https://doi.org/10.1088/1748-0221/8/01/C01020>
2. G. Anzivino et al., Precise mirror alignment and basic performance of the RICH detector of the NA62 experiment at CERN. *J. Instrum.* **13**(07), P07012 (2018). <https://doi.org/10.1088/1748-0221/13/07/P07012>
3. G. Anzivino et al., Light detection system and time resolution of the NA62 RICH. *J. Instrum.* **15**(10), P10025 (2020). <https://doi.org/10.1088/1748-0221/15/10/P10025>
4. D. Banerjee et al., The North Experimental Area at the CERN Super Proton Synchrotron. *Tech. Rep. CERN-ACC-NOTE-2021-0015*, CERN (2021). <https://cds.cern.ch/record/2774716>
5. J. Brod, M. Gorbahn, E. Stamou, Updated standard model prediction for $K \rightarrow \pi \nu \bar{\nu}$ and ϵ_K . *Proc. Sci. BEAUTY2020*, 056 (2021). <https://doi.org/10.22323/1.391.0056>
6. A.J. Buras, Standard model predictions for rare K and B decays without new physics infection. *Eur. Phys. J. C* **83**(1), 66 (2023). <https://doi.org/10.1140/epjc/s10052-023-11222-6>
7. E. Cortina Gil et al., The beam and detector of the NA62 experiment at CERN. *J. Instrum.* **12**(05), P05025 (2017). <https://doi.org/10.1088/1748-0221/12/05/P05025>
8. E. Cortina Gil et al., First search for $K^+ \rightarrow \pi^+ \nu \bar{\nu}$ using the decay-in-flight technique. *Phys. Lett. B* **791**, 156–166 (2019). <https://doi.org/10.1016/j.physletb.2019.01.067>
9. E. Cortina Gil et al., An investigation of the very rare $K^+ \rightarrow \pi^+ \nu \bar{\nu}$ decay. *J. High Energy Phys.* **2011**, 042 (2020). [https://doi.org/10.1007/JHEP11\(2020\)042](https://doi.org/10.1007/JHEP11(2020)042)
10. E. Cortina Gil et al., Measurement of the very rare $K^+ \rightarrow \pi^+ \nu \bar{\nu}$ decay. *J. High Energy Phys.* **06**, 093 (2021). [https://doi.org/10.1007/JHEP06\(2021\)093](https://doi.org/10.1007/JHEP06(2021)093)
11. E. Cortina Gil et al., HIKE, High Intensity Kaon Experiments at the CERN SPS: Letter of Intent. *Tech. Rep. CERN-SPSC-2022-031*, SPSC-I-257, SPSC-I-257, CERN, Geneva (2022). <https://cds.cern.ch/record/2839661>
12. E. Cortina Gil et al., Searches for lepton number violating $K^+ \rightarrow \pi^-(\pi^0)e^+e^+$ decays. *Phys. Lett. B* **830**, 137172 (2022). <https://doi.org/10.1016/j.physletb.2022.137172>
13. E. Cortina Gil et al., A measurement of the $K^+ \rightarrow \pi^+ \mu^+ \mu^-$ decay. *J. High Energy Phys.* **11**, 011 (2022). [https://doi.org/10.1007/JHEP06\(2023\)040](https://doi.org/10.1007/JHEP06(2023)040)
14. E. Cortina Gil et al., A search for the $K^+ \rightarrow \mu^- \nu e^+ e^+$ decay. *Phys. Lett. B* **838**, 137679 (2023). <https://doi.org/10.1016/j.physletb.2023.137679>
15. E. Cortina Gil et al., A study of the $K^+ \rightarrow \pi^0 e^+ \nu \gamma$ decay. *J. High Energy Phys.* **09**, 040 (2023). [https://doi.org/10.1007/JHEP09\(2023\)040](https://doi.org/10.1007/JHEP09(2023)040)
16. E. Cortina Gil et al., Search for dark photon decays to $\mu^+ \mu^-$ at NA62. *J. High Energy Phys.* **09**, 035 (2023). [https://doi.org/10.1007/JHEP09\(2023\)035](https://doi.org/10.1007/JHEP09(2023)035)
17. E. Cortina Gil et al., Search for K^+ decays into the $\pi^+ e^+ e^- e^+ e^-$ final state. *Phys. Lett. B* **846**, 138193 (2023). <https://doi.org/10.1016/j.physletb.2023.138193>
18. G. D'Ambrosio, A. Iyer, F. Mahmoudi, S. Neshatpour, Anatomy of kaon decays and prospects for lepton flavour universality violation. *J. High Energy Phys.* **2209**, 148 (2022). [https://doi.org/10.1007/JHEP09\(2022\)148](https://doi.org/10.1007/JHEP09(2022)148)
19. A. Diamant-Berger et al., Study of some rare decays of the K^+ meson. *Phys. Lett. B* **62**(4), 485–490 (1976). [https://doi.org/10.1016/0370-2693\(76\)90690-0](https://doi.org/10.1016/0370-2693(76)90690-0)
20. V. Fanti et al., The beam and detector for the NA48 neutral kaon CP violation experiment at CERN. *Nucl. Instrum. Methods Phys. Res. A* **574**(3), 433–471 (2007). <https://doi.org/10.1016/j.nima.2007.01.178>
21. J.R. Fry, G. Ruggiero, F. Bergsma, Precision magnetic field mapping for CERN experiment NA62. *J. Phys. G* **43**(12), 125004 (2016). <https://doi.org/10.1088/0954-3899/43/12/125004>
22. E. Goudzovski et al., Development of the kaon tagging system for the NA62 experiment at CERN. *Nucl. Instrum. Methods Phys. Res. A* **801**, 86–94 (2015). <https://doi.org/10.1016/j.nima.2015.08.015>

23. P.D. Group, R.L. Workman et al., Review of Particle Physics. Prog. Theor. Exp. Phys. **2022**(8), 083C01 (2022). <https://doi.org/10.1093/ptep/ptac097>
24. HIKE Collaboration: High Intensity Kaon Experiments (HIKE) at the CERN SPS: Proposal for Phases 1 and 2. Tech. Rep. CERN-SPSC-2023-031, SPSC-P-368, CERN, Geneva (2023). <https://cds.cern.ch/record/2878543>
25. S. Kholodenko, NA62 charged particle hodoscope. Design and performance in 2016 run. J. Instrum. **12**(06), C06042 (2017). <https://doi.org/10.1088/1748-0221/12/06/C06042>
26. A.J. Krasznahorkay et al., Observation of anomalous internal pair creation in ^8Be : a possible indication of a light, neutral Boson. Phys. Rev. Lett. **116**, 042501 (2016). <https://doi.org/10.1103/PhysRevLett.116.042501>
27. G.A. Rinella et al., The NA62 GigaTracKer: a low mass high intensity beam 4D tracker with 65 ps time resolution on tracks. J. Instrum. **14**(07), P07010 (2019). <https://doi.org/10.1088/1748-0221/14/07/P07010>

Open Access This chapter is licensed under the terms of the Creative Commons Attribution 4.0 International License (<http://creativecommons.org/licenses/by/4.0/>), which permits use, sharing, adaptation, distribution and reproduction in any medium or format, as long as you give appropriate credit to the original author(s) and the source, provide a link to the Creative Commons license and indicate if changes were made.

The images or other third party material in this chapter are included in the chapter's Creative Commons license, unless indicated otherwise in a credit line to the material. If material is not included in the chapter's Creative Commons license and your intended use is not permitted by statutory regulation or exceeds the permitted use, you will need to obtain permission directly from the copyright holder.

